

# Protein expression analysis of chronic lymphocytic leukemia defines the effect of genetic aberrations and uncovers a correlation of CDK4, P27 and P53 with hierarchical risk

Dirk Winkler,<sup>1</sup> Christof Schneider,<sup>1</sup> Manuela Zucknick,<sup>2</sup> Daniela Bögelein,<sup>1</sup> Kerstin Schulze,<sup>1</sup> Thorsten Zenz,<sup>1</sup> Julia Mohr,<sup>1</sup> Angela Philippen,<sup>1</sup> Henriette Huber,<sup>1</sup> Andreas Bühler,<sup>1</sup> Annett Habermann,<sup>1</sup> Axel Benner,<sup>2</sup> Hartmut Döhner,<sup>1</sup> Stephan Stilgenbauer,<sup>1</sup> and Daniel Mertens<sup>1,3</sup>

<sup>1</sup>Department of Internal Medicine III, University Hospital Ulm, Ulm, Germany; <sup>2</sup>Biostatistics, DKFZ, Heidelberg, Germany, and <sup>3</sup>Mechanisms of Leukemogenesis, DKFZ, Heidelberg, Germany

Citation: Winkler D, Schneider C, Zucknick M, Bögelein D, Schulze K, Zenz T, Mohr J, Philippen A, Huber H, Bühler A, Habermann A, Benner A, Döhner H, Stilgenbauer S, and Mertens D. Protein expression analysis of chronic lymphocytic leukemia defines the effect of genetic aberrations and uncovers a correlation of CDK4, P27 and P53 with hierarchical risk. *Haematologica* 2010;95(11):1880-1888. doi:10.3324/haematol.2010.025734

## Online Supplementary Design and Methods

### Cell lines

The human CLL cell line EHEB [Epstein-Barr virus (EBV)-transformed CLL] was purchased from DSMZ (Braunschweig, Germany). For EHEB, FISH analysis and *IGHV* sequencing were performed and revealed a normal karyotype and mutated *IGHV* genes, respectively. The A-T cell lines AO and ER were used as negative controls for immunoblots detecting ATM. All cell lines were cultured in RPMI 1640 medium (Seromed, Berlin, Germany) supplemented with 10% fetal calf serum (FCS) (Serva, Heidelberg, Germany).

### Western blot analyses

Immunoblotting was performed on all 185 CLL samples as described previously using antibodies specific for ATM (kindly provided by T Stankovic), P53, RB (Cell Signaling Technology Inc., Beverly, USA), CDK4, P21 (Oncogene, San Diego, USA), AKT1, MCL1, P27, PCNA (Santa Cruz Biotechnology, Heidelberg, Germany), APAF1, ARF3, BAX, CCND1/2/3, STAT6 SMAC/DIABLO, XIAP, ZAP70 (BD Biosciences, Palo Alto, USA), BCL2 (Dako, Glostrup, Denmark) and CIAP2 (Serotec, Oxford, UK).<sup>1</sup> ACTIN blots were performed to control protein content. Protein expression was quantified by densitometry using ImageJ 1.38x software. Expression levels were related to the CLL cell line EHEB as the standard for subsequent normalization of all results (*Online Supplementary Figure S1*).<sup>2</sup>

### Statistical analyses

#### Imputation of missing data

Multiple imputation was performed using the `aregImpute()` function in the R library `Hmisc`.<sup>3</sup> The results from multiple imputed data sets were combined using Rubin's method for computing point estimates and variances.<sup>4</sup>

#### Protein-protein correlations (univariate analysis and multivariate analysis after statistical imputation)

For multivariate analysis of protein expression, in particular for estimation of the joint partial correlation matrix, data were imputed. It was assumed that data are missing at random (MAR). This means that the distribution of missing values is either random, or that any non-randomness can be explained completely by the data available. The proteins with the largest proportions of missing values were excluded

from analysis (CCND3, RB, PCNA, ZAP70). Furthermore, patients who still had more than 66% of protein expression values missing after exclusion of the most incomplete proteins (i.e. more than 10 out of 15 proteins) were also excluded from the analysis. Thus, the dataset used for multivariate analysis based on multiple imputation of missing values comprised 15 out of the 19 available proteins and 139 out of the 185 patients. In this subset, all proteins had less than 50% of values missing and all patients had data available for at least five out of all 15 proteins.

The degrees of association between proteins were assessed by marginal pair-wise correlations (without data imputation) as well as by partial correlations, where for each pair of proteins we controlled for the effects of all remaining proteins and for the cytogenetic aberrations, which were included in this analysis as binary dummy variables with the normal karyotype as baseline value. The partial correlation matrix entries equal the sign-reversed entries of the off-diagonal entries of the precision matrix (i.e. the inverse of Pearson's correlation matrix), standardized by the squared root of the associated inverse partial variances.<sup>5</sup>

The partial correlation matrix is illustrated by a heatmap, where the order of the proteins is determined by a seriation method, which sorts the pairs of proteins with the strongest positive partial correlations close to the diagonal. The seriation method used<sup>6</sup> produces an optimal leaf ordering in the dendrogram with respect to minimizing the sum of the distances along the Hamiltonian path connecting the leaves in the given order. The R package "seriation" (copyright © M. Hahsler, C. Buchta and K. Hornik) was used to produce the heat map.

#### Correlation of protein expression data with hierarchical risk (continuation ratio model)

Continuation ratio models for correlation of protein expression with hierarchical risk (univariate analysis) were calculated based on the assumption of a hierarchical risk as a surrogate marker for survival (ordinality assumption), meaning that the mean protein expression rises or falls from risk level to risk level.<sup>3,7</sup> Logistic regression was used to model the conditional probabilities. In the current study, the ordinal response variable *Y* is the hierarchical risk with four categories given in the order *VH* mutated < *VH* unmutated/*V3-21* < del(11q) < del(17p).<sup>8,9</sup> Continuation ratio models were fitted individually for each protein variable as input variable *X*. Two-sided Wald tests for interaction were performed first based on the extended continuation ratio

models (based on  $\chi^2$  statistics with two degrees of freedom). Only for variables with a significant test result ( $P$  value  $<0.05$ ), was the extended continuation ratio model used in the final analysis step; for all other variables the simple continuation ratio model without interaction terms was used. A protein was deemed to have a significant effect on the hierarchi-

cal risk, if the two-sided Wald test for the variable in the final continuation ratio model had a  $P$  value less than 0.05. The Wald test was based on a  $\chi^2$  statistic with either one or three degrees of freedom, depending on whether the simple or extended continuation ratio model was used.

## References

1. Winkler D, Schneider C, Krober A, Pasqualucci L, Lichter P, Dohner H, et al. Protein expression analysis of chromosome 12 candidate genes in chronic lymphocytic leukemia (CLL). *Leukemia*. 2005;19(7):1211-5.
2. Saltman D, Bansal NS, Ross FM, Ross JA, Turner G, Guy K. Establishment of a karyotypically normal B-chronic lymphocytic leukemia cell line; evidence of leukemic origin by immunoglobulin gene rearrangement. *Leuk Res*. 1990;14(4):381-7.
3. Bender R, Benner A. Calculating ordinal regression models in SAS and S-Plus. *Biometrical J*. 2000;42(6):677-99.
4. Rubin D. *Multiple Imputation for Nonresponse in Surveys*. J Wiley & Sons, New York. 1987.
5. Whittaker J. *Graphical Models in Applied Multivariate Statistics*. John Wiley, Chichester. 1990.
6. Bar-Joseph Z DE, Gifford DK, Jaakkola T. Fast optimal leaf ordering for hierarchical clustering. *Bioinformatics*. 2001;17(1):22-9.
7. Harrell F. *Regression Modeling Strategies*. Springer-Verlag, New York. 2001.
8. Krober A, Seiler T, Benner A, Bullinger L, Bruckle E, Lichter P, et al. V(H) mutation status, CD38 expression level, genomic aberrations, and survival in chronic lymphocytic leukemia. *Blood*. 2002;100(4):1410-6.
9. Krober A, Bloehdorn J, Hafner S, Buhler A, Seiler T, Kienle D, et al. Additional genetic high-risk features such as 11q deletion, 17p deletion, and V3-21 usage characterize discordance of ZAP-70 and VH mutation status in chronic lymphocytic leukemia. *J Clin Oncol*. 2006;24(6):969-75.

**Online Supplementary Table S1.** Investigated proteins with chromosomal localization of their gene, molecular weight and functional category in alphabetical order. Protein selection was based on the gene locus and involvement in apoptosis, proliferation, DNA damage or signaling.<sup>21</sup>

Protein	Chromosomal localization of gene	Molecular weight (kDa)	Functional category	
AKT1	Murine Thymoma Viral (V AKT) Oncogene Homolog 1	14q32	60	Apoptosis regulation (inhibition)
APAF1	Apoptotic Protease Activating Factor 1	12q23	130	Apoptosis regulation (promotion)
ARF3	ADP Ribosylation Factor-3	12q13	20	Signaling
ATM	Ataxia Teleangiectasia Mutated Gene	11q22	370	DNA damage reaction
BAX	BCL2 associated X Protein	19q13	21	Apoptosis regulation (promotion)
BCL2	B Cell CLL/Lymphoma 2	18q21	26	Apoptosis regulation (inhibition)
CCND1	Cyclin D1	11q13	36	Proliferation
CCND2	Cyclin D2	12p13	35	Proliferation
CCND3	Cyclin D3	6p21	34	Proliferation
CDK4	Cyclin Dependent Kinase 4	12q14	34	Proliferation
CIAP2	Apoptosis Inhibitor 2	11q22	70	Apoptosis regulation (inhibition)
MCL1	Myeloid Cell Leukemia 1	1q21	37	Apoptosis regulation (inhibition)
PCNA	Proliferating Cell Nuclear Antigen	20p12	36	Proliferation
PI3K	Phosphatidylinositol 3 Kinase	5q13	85	Apoptosis regulation (inhibition)
P21	Cyclin Dependent Kinase Inhibitor 1A	6p21.2	21	Proliferation
P27	Cyclin Dependent Kinase Inhibitor 1B (KIP1)	12p13.1-p21	27	Proliferation
P53	Tumor protein P53	17p13.1	53	DNA damage reaction
RB	Retinoblastoma	13q14.2	110	DNA damage reaction
SMAC/DIABLO	Second Mitochondria Derived Activator of Caspase	12q24.31	22	Apoptosis regulation (promotion)
STAT6	Signal Transducer and Activator of Transcription 6	12q13	100	Signaling
SURVIVIN	Apoptosis Inhibitor 4	17q25	16	Apoptosis regulation (inhibition)
XIAP	Inhibitor of Apoptosis, X Linked	Xq25	57	Apoptosis regulation (inhibition)
ZAP70	Zeta Chain Associated Protein Kinase	2q12	70	Signaling

**Online Supplementary Table S2.** Characteristics of eight CLL patients selected for comparison of the key proteins CDK4, P27 and P53 with eight immuno-purified B cell samples from healthy donors. Patients 5-8 were used for analysis of the key proteins over the clinical course (longitudinal analysis).

Patient	Purity CD19 sorting	Age	Sex	IGHV	Karyotype
1	99.6	73	male	mutated	13q-
2	99.8	61	male	mutated	normal
3	99.4	59	male	mutated	13q bidel
4	99.3	77	female	mutated	normal
5	99.3	72	male	unmutated	11q-
6	99.8	73	female	mutated	normal
7	99.7	70	male	unmutated	13q-
8	99.7	46	male	unmutated	12q+

**Online Supplementary Table S3.** Overview of patients' samples analyzed over the clinical course (longitudinal analysis). Treatment of patients 7 and 8 did not influence protein expression substantially (equal expression of all three key proteins over time).

Patient	Sample		Treatment	
	Time point	Time from diagnosis [days]	Therapy	Time from diagnosis (day)
5	1	985	none	
	2	1257	none	
	3	1741	none	
6	1	1334	none	
	2	1754	none	
	3	2111	none	
7	1	438		
	2	605		
			fludarabine	606
			fludarabine	641
		fludarabine	669	
		fludarabine	699	
	3	760		
	4	779		
8	1	475		
	2	539		
			Humax FC	564
	3	565	Humax FC	592
	4	655		

**Online Supplementary Table S4.** Characterization of CLL samples used for assessment of the activity of the ATM kinase (tumor load: median: 95%; mean: 93%; range: 78-100%; standard deviation: 5.9%).

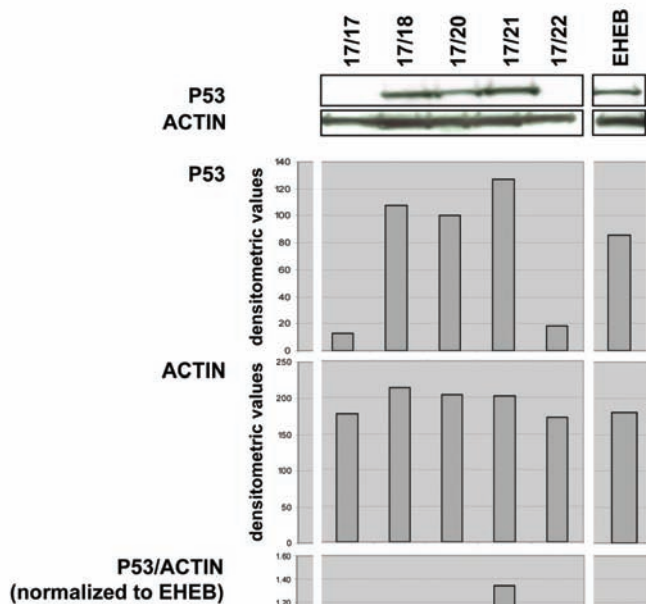
Karyotype	Tumor load (%)	Densitometric values of p-ATM induction
11q	99	26.81
11q, 12q+	91	1.30
11q, 13q	98	7.14
11q, 13q	97	41.44
11q, 13q	100	57.29
12q+	98	23.81
12q+	97	41.60
12q+	96	20.90
12q+, 13q	89	20.67
12q+, 13q	98	29.01
13q	89	14.30
13q	92	17.91
13q	94	27.79
13q	78	37.83
13q	93	27.07
13q	85	9.45

**Online Supplementary Table S5.** Description of P53 sequencing results. In order to test whether high levels of P53 protein are predictive for gene mutation even in the absence of deletion of 17p, we selected four cases without 17p deletion but strong expression of P53. In three out of four cases, a P53 gene mutation was detectable using WAVE and PCR.

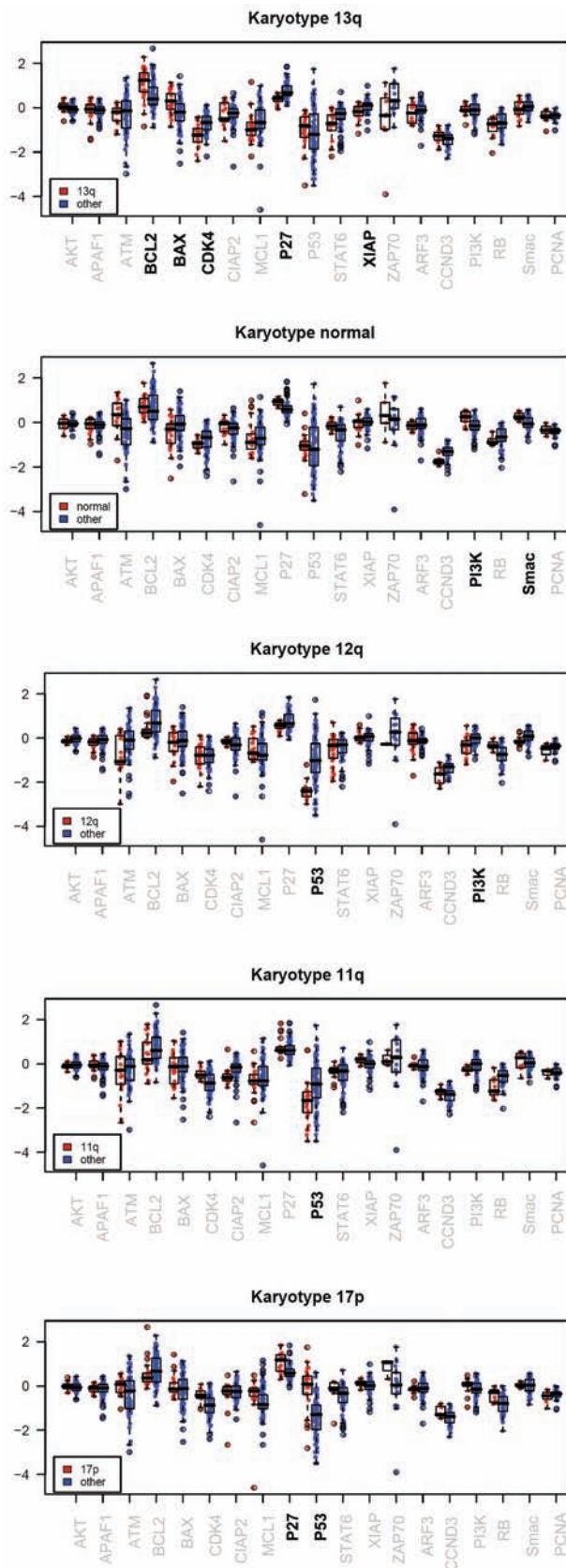
Sample	Mutation		Exon
	Wave	PCR	
Normal karyotype, IGHV unmutated	Yes	Yes	5
Normal karyotype, IGHV unmutated	Yes	Yes	10
Del(11q), IGHV unmutated	Yes	Yes	6
Del(11q), IGHV unmutated	No		

**Online Supplementary Table S6.** Measures for predictive value (Brier score) of the univariable and multivariable models. The added predictive value of the multivariable model compared to the univariable models is small: the prediction error as estimated by the Brier score only improves slightly from 0.19 to 0.17. The Brier score is a measure for the prediction error. It can take values from 0 (perfect prediction) to 0.25 for a non-informative model.

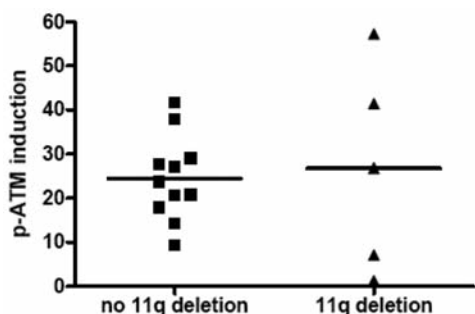
Protein	Brier score
CDK4	0.206
P27	0.191
P53	0.207
multivariable	0.170



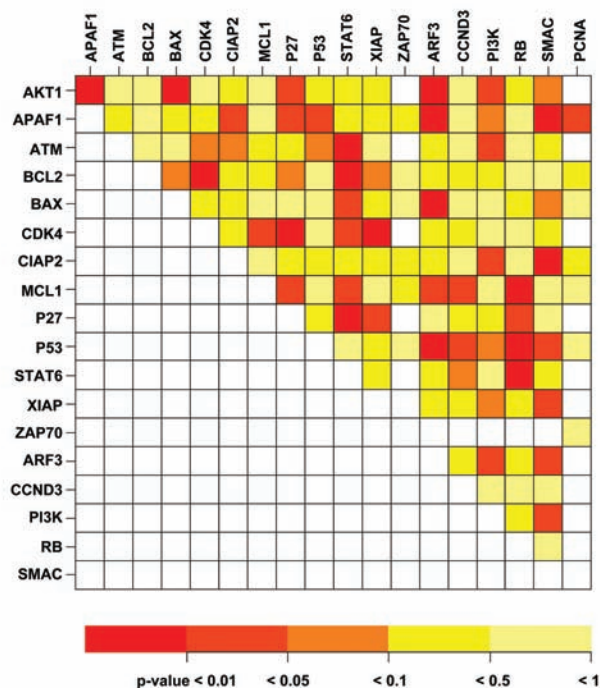
Online Supplementary Figure S1. Example of protein expression quantification by densitometry for P53. Measured densitometric values (y-axis) of protein expression were first normalized to levels of actin and then related to expression levels in EHEB cells.



Online Supplementary Figure S2. Combined box plots and dot plots comparing patients with a specific karyotype (red dots) versus all patients without this karyotype (blue dots). The karyotype order reflects the hierarchical model proposed by Döhner and colleagues.<sup>1</sup> Proteins that were differentially expressed after adjustment for multiple testing are highlighted with bold letters. Each dot represents a single CLL case. Negative values of expression (y-axis) are the result of log-transformation for statistical analysis. For *P* values and patient numbers see text.



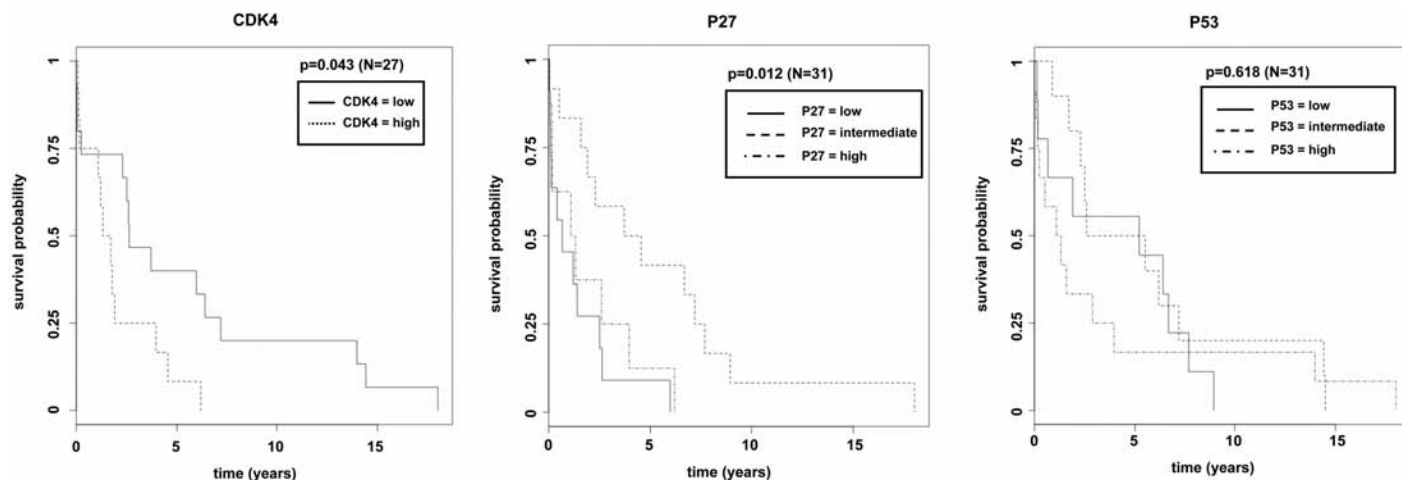
Online Supplementary Figure S3. Induction of phospho-ATM following 5 Gy ionizing radiation in CLL cases with (N=5) and without (N=11) del(11q). Induction of phospho-ATM was independent of the presence of del(11q). For sample characterization please see Online Supplementary Table S4.



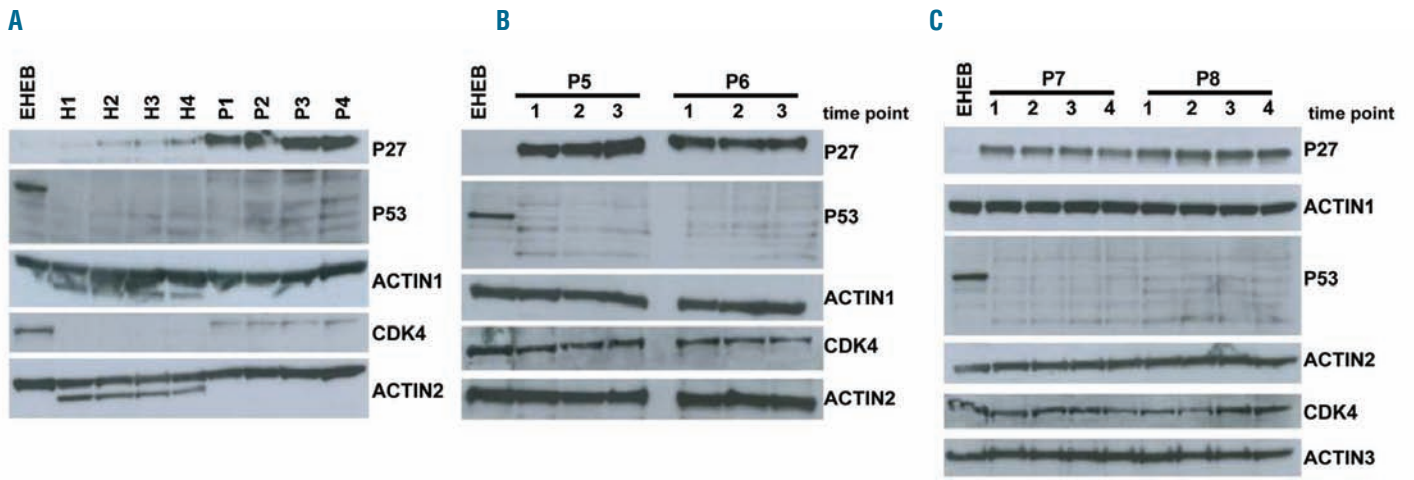
Online Supplementary Figure S4. Heat map showing results of pairwise protein-protein correlations (univariate analysis on non-imputed data set). Please note that the colors reflect the P value. The strongest correlations with adjusted P values are listed in Table 2.



Online Supplementary Figure S5. Bubble graph illustrating the indirect negative correlation between AKT1 and STAT6 (correlation coefficients: STAT6/ARF3: 0.22; ARF3/AKT1: -0.21).



Online Supplementary Figure S6. Kaplan-Meier curves for treatment-free survival from diagnosis stratified by protein expression levels (high:  $\log(\text{expression}) > \text{median}$ , low:  $\log(\text{expression}) \leq \text{median}$  for CDK4). The relations between treatment hazard and P53 as well as P27 protein expression levels show a slight non-linear effect. Therefore Kaplan-Meier plots with three strata (cut-offs at the 33%-quantile and 67%-quantile) were used. For P53 no statistically significant separation of the three groups was seen. The given P values correspond to the log-rank tests between these groups.



**Online Supplementary Figure S7.** Most key proteins differ in expression pattern between CLL cells and non-malignant B cells but are generally stable during the course of the disease. (A) Comparison of the expression pattern of P27, P53 and CDK4 between four different non-malignant B cell samples (H1-H4) and four different CLL cell samples (P1-P4). EHEB cell lysate serves as a positive control for P53 and CDK4 expression. (B) Expression level analysis of key proteins during the course of disease (time point 1-3) in two untreated patients (P5, P6). (C) Expression level analysis of key proteins during the course of the disease (time points 1-4) in two treated patients (P7, P8). For CLL sample characterization and treatment please see *Online Supplementary Tables S2 and S3*.